ACS APPLIED MATERIALS & INTERFACES

Research Article

www.acsami.org

Highly Thermostable, Flexible, and Conductive Films Prepared from Cellulose, Graphite, and Polypyrrole Nanoparticles

Jinghuan Chen,[†] Jikun Xu,[†] Kun Wang,*[,†] Xueren Qian,[‡] and Runcang Sun*[,†]

[†]Beijing Key Laboratory of Lignocellulosic Chemistry, Beijing Forestry University, Beijing 100083, China

[‡]Key Laboratory of Bio-Based Material Science and Technology of Ministry of Education, Northeast Forestry University, Harbin 150040, China

Supporting Information

ABSTRACT: In this study, graphite powder (GP) was introduced into the conductive cellulose/polypyrrole (PPy) composite films to increase their conductivity and thermal stability. The GP was dispersed in ionic liquid 1-butyl-3-methylimidazolium chloride ([Bmim]Cl) before the dissolution of cellulose, and the cellulose/GP/PPy films were prepared by in situ chemical polymerization of PPy nanoparticles on the film surface. The structural characteristics and properties of the composite films were investigated in detail. The GP flakes, which were embedded in the cellulose matrix, increased the thickness and decreased the density of the films, leading to the decrement of mechanical properties. However, the thermal stability of the films was significantly improved by the incorporation of graphite, and the composite film could even substantially maintain the original shape after being burned. In addition, the electrical conductivity of the films was increased seven times, leading to the excellent electromagnetic interference shielding effectiveness. The cellulose/GP/PPy film could be considered as a potential candidate for the effective lightweight electromagnetic interference shielding materials in electronics, radar evasion, aerospace, and other applications.

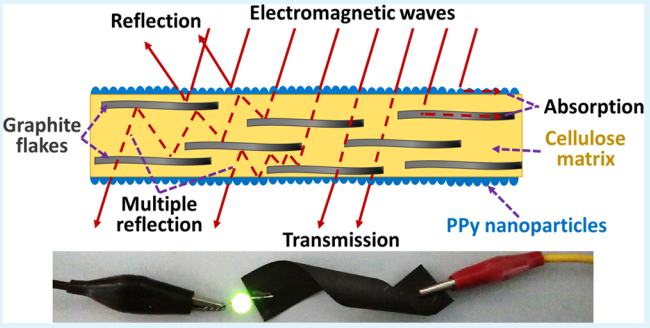

KEYWORDS: *cellulose, graphite, polypyrrole, thermal stability, conductive film*

1. INTRODUCTION

The discovery of conductivity polymers demonstrated that organic polymers are substitutes for semiconductors and metallic conductors.[1] The most promising conductive polymers, including polythiophene (PT), polyaniline (PANI), polypyrrole (PPy), poly(3,4-ethylenedioxythiophene) (PEDOT) and poly phenylenevinylene (PPV), have been used in the applications of sensors, bioelectronics, energy storage devices, dye-sensitized solar cells, CO_2 capture and water treatment materials, due to their relatively high electron conductivity and stability in oxidized state.[2−6] Among the available conductive polymers, PPy has attracted significant attention because of its facile synthesis in both organic and aqueous media, excellent ion-exchange properties, good electroconductibility at room temperature (varying from 10^{-4} to 10^{2} s cm^{-1}) and the ability to efficiently switch between the redox states.[7] PPy film can be prepared from electrochemical polymerization of pyrrole (Py); however, it is not feasible for large-scale applications due to the limited area of electrodes.[8] The oxidative chemical polymerization of Py in aqueous or nonaqueous media commonly employed ferric chloride ($FeCl_3$) as an oxidant and doping agent.[9] The obtained PPy powder is normally brittle, indissoluble in most solvents, and hard to be compacted or heat annealed, leading to the poor mechanical properties and processability. Therefore, Py is often directly polymerized on various substrate materials to overcome these problems.[10]

In recent years, composites materials based on conductive polymers and cellulose have aroused great interest because of the environmental friendliness and cost effectiveness of cellulose.[11] As the most abundant natural polymer on earth, cellulose can be derived from annual plants, agricultural byproducts, and woods. Due to the development of solvents for cellulose, the intermolecular and intramolecular hydrogen bonds between cellulose chains can be destroyed and rearranged to form membrane, film, fiber, hydrogel, aerogel, and other materials. Various forms of cellulose, such as filter paper,[12] wood cellulose fibers,[13] bacterial cellulose,[14] nanofibrillated cellulose,[11] nanocrystal cellulose,[15] cellulose aerogels,[16] and cellulose derivatives,[17,18] have been used as templates and coated with PPy by in situ oxidative polymerization or chemical vapor deposition to prepare conductive composites for self-powered drug delivery,[19] energy storage,[20−22] nerve regeneration,[16] and other applications.[18] These materials combine the electrical properties of conductive polymers with the unique properties of cellulose. In addition,

Received: May 22, 2015
Accepted: July 2, 2015
Published: July 2, 2015

DOI: 10.1021/acsami.5b04462
ACS Appl. Mater. Interfaces 2015, 7, 15641−15648

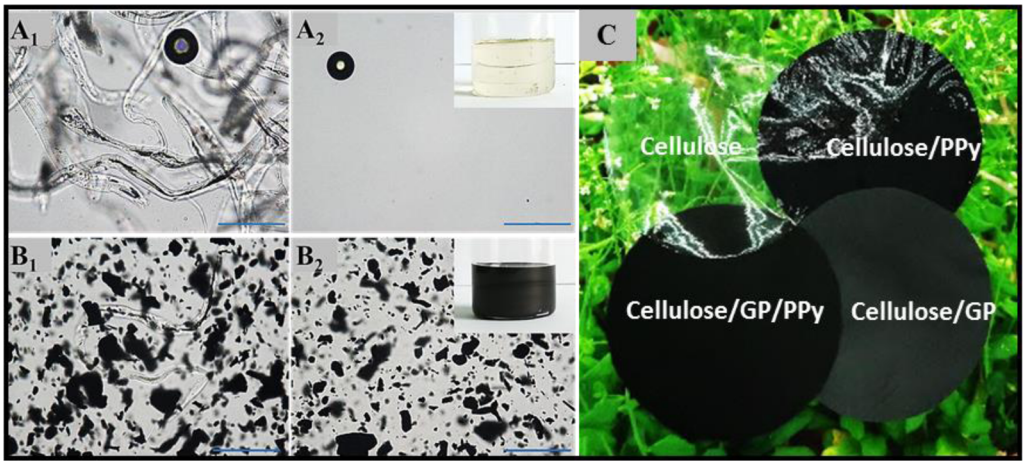

Figure 1. Optical microscopic images of cotton linter pulp before and after being dissolved in (A_1, A_2) [Bmim]Cl and (B_1, B_2) [Bmim]Cl/graphite (GP); (insets) digital photos of the solutions (scale bar, 50 um); and (C) the digital photos of the obtained films.

special chemicals can be added into the cellulose/PPy composites to induce extra performance. For example, the incorporation of silver nanoparticles improved the antimicrobial property of cellulose/PPy composite,[23] and the coating of active metals on the drug-contained PPy-cellulose film made the drug autonomously released.[19]

In this work, graphite powder (GP) was introduced into cellulose/PPy films to increase their conductivity and thermal stability. The GP was added before the dissolution of cellulose in ionic liquid, 1-butyl-3-methylimidazolium chloride ([Bmim]-Cl), and PPy was then synthesized on the surface of the casted and regenerated cellulose/GP film through the vapor-phase deposition process. The structural characteristics of the obtained composite films were investigated by X-ray diffraction (XRD), Fourier transform infrared (FTIR) spectra, scanning electron microscopy (SEM), and atomic force microscopy (AFM). The mechanical properties, thermal stability, conductivity and electromagnetic interference shielding effectiveness of the composite films were also studied in detail. This study provided a promising method to improve the thermal stability and conductivity of the cellulose/PPy composite films.

2. EXPERIMENTAL SECTION

2.1. Materials. Cotton linter pulp with α-cellulose content of more than 95% was supplied by Hubei Chemical Fiber Co. Ltd. (Hubei Province, China). Its weight-average molecular weight (M_w = 768 810 Da) and number-average molecular weight (M_n = 342 790 Da) were determined by gel permeation chromatography (GPC; Agilent 1200 series, Santa Clara, CA) according to a previous literature procedure.[24] GP with particle size of 300 mesh was purchased from Sinopharm Chemical Reagent Co., Ltd. (Shanghai, China). Pyrrole monomer (Py, 98%) was also purchased from Sinopharm Chemical Reagent Co., Ltd., and purified by vacuum distillation before use. The ionic liquid, [Bmim]Cl (purity ≥99%), was purchased from Lanzhou Institute of Chemical Physics (Lanzhou, China) with a water content of less than 0.9%. Ferric chloride ($FeCl_3$) and other chemicals were of analytical grade and used without further purification. The PPy powder was prepared by polymerization of Py in $FeCl_3$ aqueous solution according to a previous method.[20]

2.2. Preparation of Cellulose/GP Composite Films. First, 19.2 g [Bmim]Cl was added into a three-necked glass flask (50 mL) equipped with a mechanical stirrer, and heated at 100 °C with an oil bath under nitrogen atmosphere until a homogeneous solution was formed. Certain amount of GP (0, 0.08, 0.24, 0.4, 0.56, 0.8, 1.04, 1.28, and 1.6 g, respectively) was dispersed in the solvent by vigorous stirring for 20 min. Then, 0.8 g cotton linter pulp was carefully added into the mixture at 100 °C with further stirring until the pulp was completely dissolved. The obtained mixture was degassed under vacuum and then casted on a glass plate with a thickness of 0.56 mm. The plate was briefly placed in an oven at 70 °C to smooth the surface and then immediately immersed into a water bath at room temperature to coagulate and regenerate. After being washed several times with water, the regenerated film was sandwiched between filter papers and pressed under a certain pressure to remove the water and prevent shrinkage. The filter papers were replaced several times until the GP-cellulose composite film was dried. The obtained films were labeled as C_0, C_{10}, C_{30}, C_{50}, C_{70}, C_{100}, C_{130}, C_{160}, and C_{200}, respectively, in which the subscript represents the percent of GP based on the weight of cotton linter pulp in the film.

2.3. In Situ Chemical Deposition of PPy on Cellulose/GP Films. The cellulose/GP composite films were impregnated in 2.0 mol/L $FeCl_3$ aqueous solution for 1 h, and then exposed to Py vapor in equilibrium with Py liquid inside a vacuum vessel. After the in situ polymerization for 10 min under reduced pressure (−0.1 MPa), the films were removed from the vessel and washed throughout with acetone and water. The films were then subjected to ultrasound for 5 min to remove the dissociative and loosely bound PPy, followed by being sandwiched between filter papers to dry as mentioned above. The films were labeled as P_0, P_{10}, P_{30}, P_{50}, P_{70}, P_{100}, P_{130}, P_{160}, and P_{200}, respectively, and conditioned at 65% relative humidity (RH) and 20 °C for 24 h before the performance testing. (The preparation process of the composite films is shown in the Supporting Information Figure S1).

2.4. Characterization. The XRD patterns of the films were measured on a XRD-6000 instrument (Shimadzu, Japan) with Ni-filtered CuKα radiation (χ = 1.542 Å) generated at 40 kV and 30 mA, and recorded from 5 to 60° (2θ) with a scanning speed of 0.2°/min. The FTIR spectra of the composite films were carried out on a Thermo Scientific Nicolet iN10 FTIR Microscope (Thermo Nicolet Corp., Madison, WI) in the mode of attenuated total reflection (ATR) with a pressure control accessory, and recorded in the range from 4000 to 670 cm^{-1} with 128 scansions per sample at a resolution of 4 cm^{-1}.

The morphologic characteristics were observed by a Hitachi S-3400N scanning electron microscopy (Hitachi, Japan) at acceleration voltages of 5 kV. The films were sputtered with gold using a sputter coater (E-1010, Hitachi, Japan) prior to the examination. The three-dimensional (3D) nanoscale topography of the film surface was measured using a Nanoscope IIIa multimode scanning probe microscope (Digital Instruments, Inc., Tonawanda, NY). The AFM images were scanned using tapping mode regime in air at room temperature with silicon cantilevers. The images were only flattened without any other processing.

2.5. Performance Testing. The thickness of the films was measured with a digital caliper, and the measurement was carried out

DOI: 10.1021/acsami.5b04462
ACS Appl. Mater. Interfaces 2015, 7, 15641−15648

at 10 different positions of the film. The tensile strength, elongation at break, and initial modulus of the films were tested using a universal tensile tester (UTM6503, Shenzhen Suns Technology Stock Co., Ltd., China). The wet strength of the films were measured at the same conditions after the films being soaked in water for 1 h.

The electrical resistivity of the films was measured by a RTS-8 four-point probe system (Shenzhen Four Probes Tech Co. Ltd., China) with copper electrodes arranged in a straight line. To control the moisture content of the conductive films and make the results comparable, the films were preconditioned at 20 ± 1 °C and 67% relative humidity (RH) for 24 h and measured at the same environment. The average electrical resistivity was calculated from 10 measurements from both front and back side, and the conductivity was computed using $\sigma = 1/\rho$.

The amount of PPy deposited on the film surface, expressed as A (g/m^2) was determined according to the following equation:

$$A = \frac{W - W_0}{S} \quad (1)$$

where, W_0 and W are the weight of the film before and after PPy deposition, and S is the surface area of the film.

The electromagnetic interference (EMI) shielding effectiveness (SE) of the films were measured at room temperature in the frequency range of 30 MHz to 1.5 GHz on a flanged coaxial electromagnetic interference shielding effectiveness tester (DR-S02, EMC Technology Company, China) and a vector network analyzer (NA7300A, Deviser Company, China) according to the method of ASTM D 4935−10.

The thermal properties of the films were investigated by thermogravimetric analyses (TGA). The TGA measurements were performed on DTG-60 (Shimadzu, Japan) simultaneous DTA-TG apparatus at a heating rate of 10 °C/min from 40 to 800 °C under inert nitrogen gas atmosphere. The flame resistance test of the films was carried out by directly burning the films for 10 s in the flam of alcohol burner, referring to the standard test method EN ISO 15025. The state of the films during burning process was recorded by photographs.

3. RESULTS AND DISCUSSION

[Bmim]Cl is a nonderivative solvent for cellulose.[25] The cotton linter pulp could be completely dissolved in [Bmim]Cl even with the dispersed GP (Figure 1,A,B), indicating that the addition of GP had no effect on the dissolution of cellulose. In addition, nearly no isolated GP particles were found in the coagulating bath or washing water during the spinning process, suggesting that the GP particles were almost completely trapped within the regenerated cellulose network. The obtained cellulose film was colorless and transparent, while the cellulose/GP composite film was gray and opaque. The black films were finally obtained after the in situ chemical deposition process, confirming the successful polymerization of PPy. In comparison, the cellulose/PPy film exhibited a glossy surface, and the cellulose/GP/PPy composite film had a rough surface, probably due to the incorporation of GP (Figure 1,C).

3.1. Chemical Structure and Morphology of the Composite Films. The typical XRD pattern of cellulose II was clearly reflected in the cellulose film (C_0; Figure 2).[26] In comparison, the pure PPy powder had a broad diffraction peak around 26.6°, signifying an amorphous phase.[21] The cellulose/PPy composite film (P_0) exhibited a similar XRD pattern to PPy, and the peaks for cellulose almost disappeared, implying the complete coating of PPy on the surface of cellulose. The strong diffraction peaks of GP were observed at 23.9, 26.5, and 54.6°, in which a clear shift of the peak at 26.5−26.2°, corresponding to the (002) diffraction plane of GP, was detected in C_{200} and P_{200}, indicating the successful preparation of the composite films.[27]

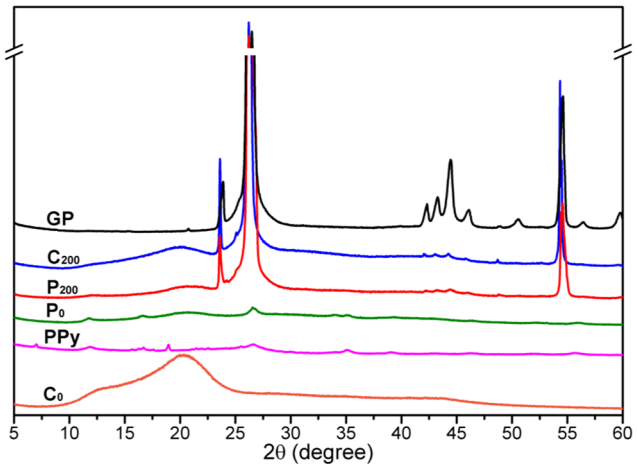

Figure 2. XRD patterns of GP, PPy powder, cellulose film (C_0), cellulose/PPy film (P_0), cellulose/GP film (C_{200}), and cellulose/GP/PPy film (P_{200}).

The FT-IR spectra of the cellulose film (C_0) exhibited the characteristic absorption of cellulose (Figure 3),[28] and the

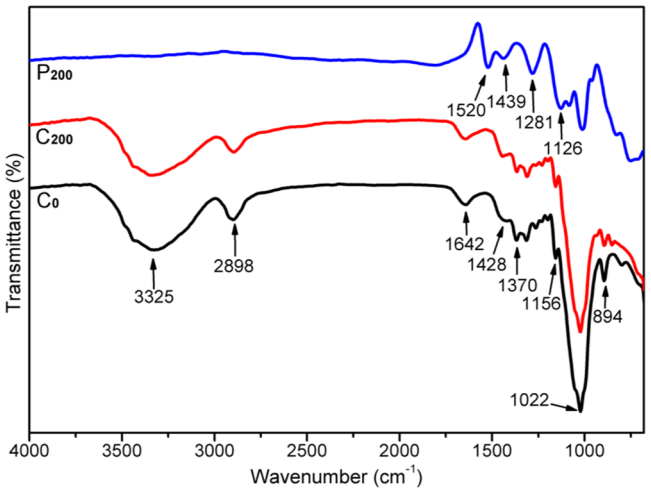

Figure 3. FT-IR spectra of the films C_0, C_{200}, and P_{200}.

similar spectrum of film C_{200} was also observed, suggesting that the characteristic peaks of GP were overlapped and difficult to be identified. For the film P_{200}, the peak at 1520 cm^{-1} is assigned to a mixed C=C and inter-ring C−C vibration of PPy units, and the peak at 1439 cm^{-1} is related to C−N stretching vibration in the Py ring. The other two typical peaks of Py, one at 1281 cm^{-1} for the C−H in-plane ring bending modes and another at 1126 cm^{-1} for the C−N in-plane ring deformation and bending modes, were also clearly classified. In contrast, the characteristic absorptions of cellulose in film P_{200} are weakened or almost disappear, indicating that the film was completely wrapped by PPy. No new peaks were observed from the composite films, suggesting that no new chemical bonds were formed between them during the synthesis process.

From the morphological analysis, the cellulose/PPy film (P_0) showed the flat surface and compact cross-sectional structure, while the films P_{10}, P_{50}, P_{100}, and P_{200} were rough and had a layered structure (Figure S2, SI). GP flakes with size of several tens of microns could be clearly observed on the surface and in the interior of these films, indicating that the GP flakes were

DOI: 10.1021/acsami.5b04462
ACS Appl. Mater. Interfaces 2015, 7, 15641−15648

not removed during the coagulating and washing processes, probably ascribing to the connections between GP and cellulose. In addition, the thickness of the obtained films were only 10−100 μm, although all the solutions were casted with a fixed thickness of 560 μm. This phenomenon could be probably attributed to the removal of solvents and the recombination of cellulose chains during the regenerating and drying processes. The addition of GP flakes raised the concentration of the solutions and hindered the recombination of some cellulose chains, resulting in the thickness of the composite films increasing with the increasing content of GP. According to the high-magnification SEM image for the cross section of composite film P_{200} (Figure 4a), the GP flakes were embedded in the cellulose matrix. The voids in the film certainly resulted from the bending and curling of GP flakes since the complete dispersion of GP flakes was hardly realized in [Bmim]Cl solvent with high viscosity. This distribution of GP also influenced the mechanical and conductive properties of the films, which will be discussed later. It can be also observed that the film surface was covered uniformly with small particles. The nanoscale topography for the surface of the cellulose film (C_0) and cellulose/GP/PPy film (P_{200}) were investigated by AFM (Figure 4b,c). The surface of C_0 revealed lots of nanopores with a diameter less than 100 nm, which was supposed to be formed during the diffusion of ionic liquid and water in the coagulation bath. The surface of P_{200} (Figure 4c) was covered by nanoparticles around 100 nm in diameter. Combining with the results from FT-IR analysis, these nanoparticles are PPy synthesized by the chemical vapor deposition method. Although the PPy nanoparticles filled the pores on cellulose film surface, the roughness RMS (R_q) value of film P_{200} surface (22.5 nm) was much higher than that of C_0 (3.96 nm), confirming that the incorporation of GP flakes decreased the surface smoothness of the cellulose films.

3.2. Mechanical and Thermal Properties. PPy conductive polymer has poor mechanical integrity and is hard to be shaped, which could be overcome by the utilization of cellulose template.[16] Direct synthesis of PPy on the surface of cellulose template is a low-polluting process to improve the mechanical properties.[29] In this study, the cellulose/PPy composite film has high mechanical properties due to the robust cellulose film substrate. However, the tensile strength, and Young modulus of these films were significantly decreased from 158 to 66 MPa and 3.4 to 1.6 GPa, respectively, with the increasing GP content from 0 to 30 wt % (based on the mass of cellulose; Table 1). As the content of GP was increased to higher than 30 wt %, the downward trend of tensile strength and Young's modulus of the composite films was slowed down. In comparison, the elongation at break of the composite films was linearly decreased with the increase of GP content. These mechanical properties of the composite films were probably related to the stiffness of the GP flakes and the weak connection between GP flakes and cellulose. As it had been reported that few hydroxyl groups are existed on the surface of GP flakes,[30] the incorporation of GP flakes into the cellulose matrix destroyed the compact cellulose hydrogen bond network, which led to the decrement of film strength. Meanwhile, the elongation at break of the films was decreased due to the inextensibility of GP flakes. However, the mechanical properties of these composite films were comparable to the graphene oxide/cellulose carbamate composite films (tensile strength of 27−78 MPa and Young's modulus of 0.35−1.56 GPa),[31] which was probably attributed to the compact structure of the cellulose

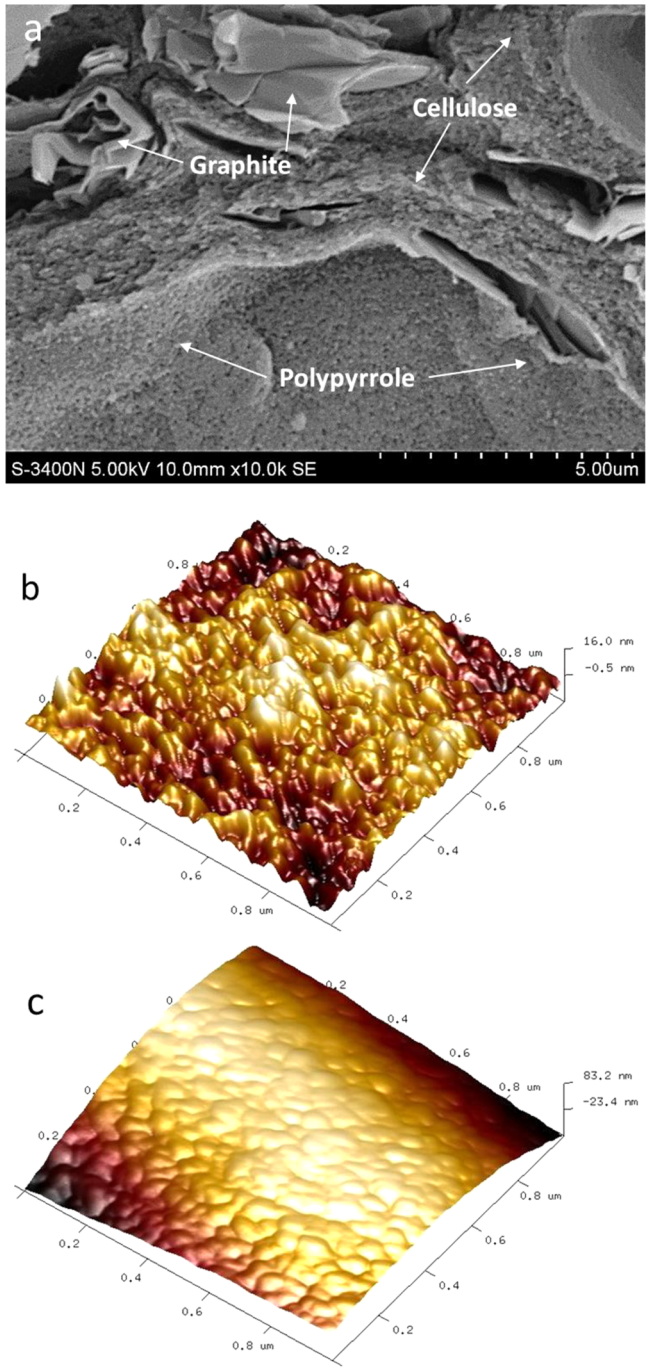

Figure 4. (a) Enlarged cross-sectional SEM image of film P_{200}, and the AMF images for the surface of film (b) C_0 and (c) P_{200}.

matrix. Additionally, the wet strength of composite films was also measured after being soaked in water for 1 h (Table 1). Although the tensile strength and Young's modulus of the films were decreased, the values of elongation at break were significantly increased. With the increment of GP content in the films, the retention rate of strength in wet condition increased from 20.4% (P_0) to 49.4% (P_{200}), while the rate of increase in elongation at break was lowered down from 3.5 times (P_0) to 1.0 times (P_{200}), suggesting that the incorporation of GP could help to increase the wet strength of the films. Furthermore, the cellulose/GP/PPy composite film could be washed in water like cloth without any dissociation (Supporting Information, Video S1), illustrating its excellent laundry-

DOI: 10.1021/acsami.5b04462
ACS Appl. Mater. Interfaces 2015, 7, 15641−15648

Table 1. Tensile Strength, Elongation at Break and Young's Modulus of the Cellulose/GP/PPy Films with Different Contents of GP in Dry and Wet Conditions

	mechanical property in dry condition[a]			mechanical property in wet condition		
samples	σ_b (MPa)	ε_b (%)	E (GPa)	σ_b (MPa)	ε_b (%)	E (GPa)
P_0	158.0 (5.1)[b]	10.6 (0.7)	3.36 (0.13)	32.2 (2.7)	37.5 (4.6)	0.44 (0.06)
P_{10}	90.8 (4.8)	10.0 (0.5)	2.30 (0.10)	26.7 (2.4)	33.9 (3.2)	0.53 (0.08)
P_{30}	66.4 (4.2)	9.4 (0.6)	1.63 (0.08)	21.9 (2.2)	23.4 (3.8)	0.71 (0.06)
P_{50}	61.9 (4.1)	7.2 (0.6)	1.43 (0.06)	18.5 (1.9)	14.8 (3.3)	0.84 (0.07)
P_{70}	42.8 (3.9)	6.0 (0.5)	1.06 (0.06)	14.3 (1.7)	8.6 (2.9)	0.46 (0.05)
P_{100}	36.7 (3.6)	5.2 (0.5)	1.22 (0.08)	11.7 (2.3)	7.4 (2.6)	0.72 (0.08)
P_{130}	34.3 (3.5)	4.0 (0.4)	1.30 (0.08)	13.7 (1.8)	6.3 (2.1)	0.56 (0.06)
P_{160}	32.7 (3.6)	3.9 (0.5)	17.06 (0.07)	12.9 (1.6)	4.5 (1.8)	0.58 (0.06)
P_{200}	23.7 (3.2)	3.3 (0.4)	1.01 (0.06)	11.7 (1.2)	3.4 (1.6)	0.67 (0.07)

[a] σ_b, ε_b, and E are the tensile strength, elongation at break, and Young's modulus of the composite films under stretching model, respectively. [b] Values in parentheses are the standard errors.

resistance. Therefore, these conductive composite films have much wider applications as compared with the traditional conductive papers.

From the thermogravimetric analyses of the materials and films (Figure 5), the GP powder showed no weight loss until the temperature reached to 600 °C, and the residual weight was more than 75% after being experienced to 800 °C, indicating the excellent thermal stability. The significant weight loss (about 70%) of film C_0 was occurred around 300−350 °C. However, the weight loss of film C_{50} and C_{200} in the same temperature range were reduced to 50 and 22%, respectively, due to the addition of GP to cellulose matrix. The thermal degradation of PPy powder could be divided into three stages:[20] the low-molecular weight Py oligomers and water were first released below 100 °C; the counterions were degraded between 100 and 315 °C; the degradation of PPy backbone was occurred above 315 °C, and half of the weight was remained at 800 °C. The chemical deposition of PPy on the surface of cellulose and cellulose/GP composite films reduced the onset degradation temperature from 300 to around 200 °C, which was probably attributed to the interactions between cellulose and PPy.[32] However, it is noteworthy that the thermal stability of the composite films was greatly improved by coating PPy. No weight loss was obviously observed throughout the heating process, and the final residue weights were increased by 15−40%. This could be probably attribute to the dense carbon char layer formed by the thermal degradation of PPy coating, which might prevent the decomposition of cellulose and graphite at high temperature and promote the heat transfer of the films, leading to the improvement of thermal stability.

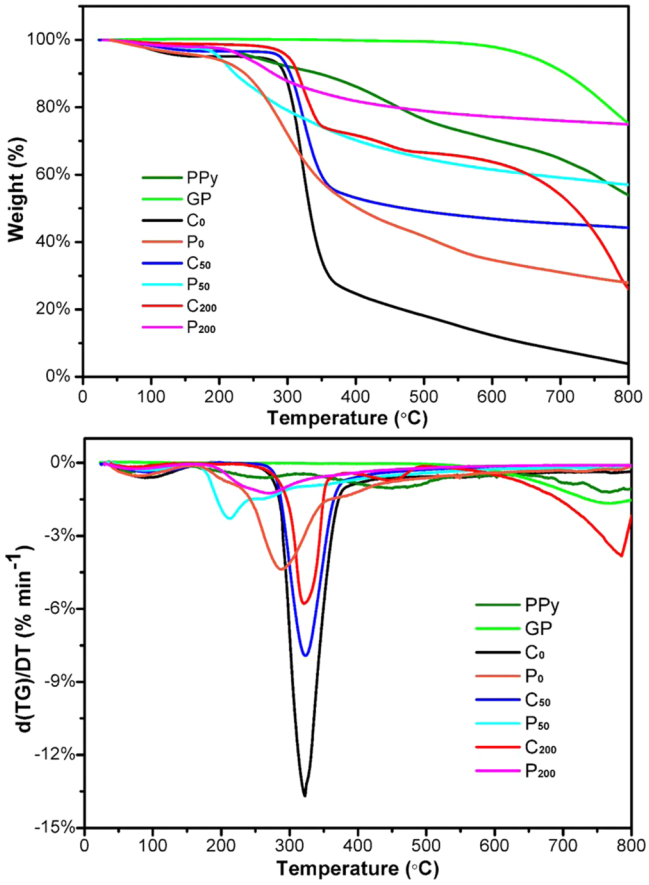

Figure 5. TGA/DTG analysis of the PPy, GP, C_0, and composite films P_0, C_{50}, P_{50}, C_{200}, and P_{200}.

The flame resistance test was conducted by burning the films in flame for 10 s (Figure 6). PPy has been extensively used as an effective antiflammable coating for cotton, silk, PET and epoxy resin to improve the flame resistance of these substrates.[33−35] This improvement was probably attributed to the high stability of the conjugated structure of PPy backbone and the strong interaction between PPy and substrates.[36] In this study, the film P_0 was only shrunk without being burned into ashes, indicating that PPy is a good flame retardant. The natural GP flake also has excellent thermal properties due to its preferential crystalline orientation and high degree of graphitization,[37] and it has been used to enhance the thermal properties of paraffin/polyethylene composite materials and polyurethane nanofibers.[38,39] However, the film C_{200} with 200% GP addition was finally burned into fragments, which was probably ascribe to the fact that the GP flakes were embedded in the cellulose matrix and dropped out as cellulose was completely thermal degraded. It is worth noting that the film P_{200} was able to substantially maintain the original shape after being burned, indicating that the PPy coating acted as a protective layer, which isolates the oxygen, inhibits the thermal degradation of cellulose and prevents the fragmentation of GP. Therefore, these composite films could be used in wider applications due to their flame-retardant, heat-shielding and not melting characteristics.

DOI: 10.1021/acsami.5b04462
ACS Appl. Mater. Interfaces 2015, 7, 15641−15648

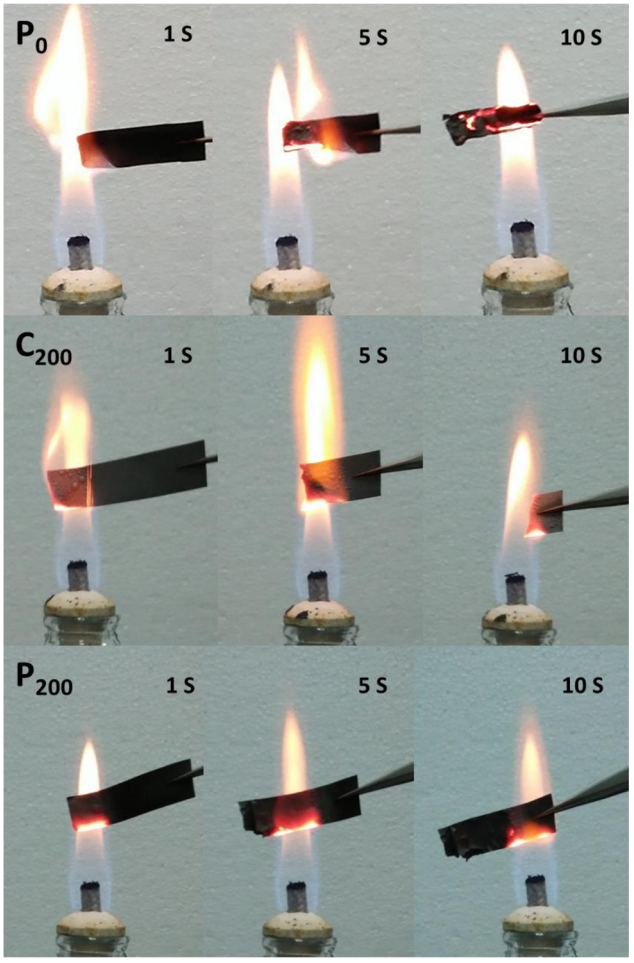

Figure 6. Photographs of the films P_0, C_{200}, and P_{200} after being burned for 1, 5, and 10 s.

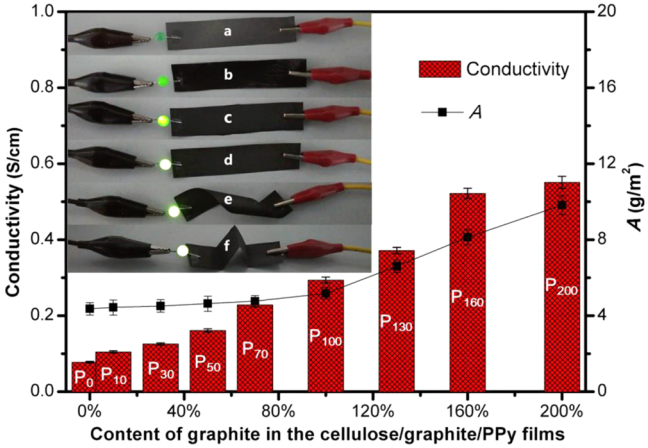

Figure 7. Conductivity and the amount of deposited PPy (A) on the composite films with different contents of GP, inset is the lighting of an LED using film (a) C_{200}, (b) P_0, (c) P_{50}, and (d–f) P_{100} as part of the wire.

3.3. Electoral Conductivity and Electromagnetic Interference Shielding Effectiveness. As known, cellulose was nonconductive materials and GP has good electrical conductivity. However, in this study, the electroconductibility of the cellulose/GP composite films were not improved by the addition of GP. As intuitively reflected in the inserted photo images in Figure 7, the light emitting diode (LED) lamp was not bright when a portion of the wire was replaced by the cellulose/GP film C_{200}. The probable reason for the high resistivity of the composite film was that the GP flakes were isolated and wrapped by the cellulose network matrix (Figure 4a), and this discontinuity of the GP flakes hindered the conduction of electrons. Clearly, the chemical deposition of PPy significantly increased the electrical conductivity of the composite films. During the polymerization of PPy, $FeCl_3$ is used both as an oxidant and a dopant. The Fe(III) oxidizes the Py monomer to a radical monomer, which could be rapidly coupled to form a dimer, and PPy chains are finally formed by the deprotonation of bipyrrole and the chain propagation.[40] Meanwhile, the Cl^- acts as a doping ion, which incorporates into the PPy and lowers the boundary π-levels of the PPy backbone by removing the π-electrons from the upper zone of the valence band, leading to the conductivity of PPy.[41] Thereby, the LED lamp was faintly lighted with taking the cellulose/PPy film (P_0) as part of the wire. Due to the lightweight, conductive and porous structure of GP, PPy/GP composites have been prepared to enhance the conductive performance.[42,43] In this study, the conductivity of the cellulose/GP/PPy composite films were increased with the increasing content of GP. The film with 10% GP (P_{10}) had a conductivity of 0.10 S cm^{-1}, and which increased to 0.55 S cm^{-1} as 200% GP was added (P_{200}). It should be pointed out that the increment of the conductivity could not be attributed to the conductivity of GP, because the GP flakes were discontinuous in the composite films just as discussed above. However, the SEM and AFM images (Figure S1, SI, and Figure 4) revealed that the GP flakes increased the roughness of the cellulose/GP composite films, thus it is reasonable to assume that more $FeCl_3$ could be reserved on the cellulose/GP film surface during the soaking process, promoting the deposition of PPy. This has been confirmed by measuring the amount of deposited PPy, which gradually increased from 4.3 to 9.8 g/m^2 with the GP content from 0 to 200% (Figure 7). The conductivities of the obtained cellulose/GP/PPy composite films are comparable to the PPy coated conductive paper prepared by vapor-phase method (about 0.5 S cm^{-1})[12] and the cellulose/PPy conducive paper composite prepared by in situ polymerization method (about 0.3 S cm^{-1}).[13] Furthermore, the cellulose/GP/PPy composite films had excellent flexibility. The film even with a GP content of 100% (based on the weight of cellulose) could be twisted and folded without damage, and the LED lamp flashed well under these conditions.

From the electromagnetic interference shielding effectiveness (EMI SE) test of the films (Figure 8a), the cellulose film C_0 showed no electromagnetic shielding performance, which was significantly improved by the addition of GP. When the content of GP increased from 100 to 200%, the EMI SE of the cellulose/GP films raised from 7 to 18 dB. This improvement was attributed mainly to the excellent electromagnetic shielding performance of GP, which has been widely used to prepare efficient electromagnetic interference shielding materials.[44,45] The EMI SE of these films was further improved by the surface chemical deposition of PPy. The cellulose/PPy film P_0 had an EMI SE of around 12 dB and the cellulose/GP/PPy film P_{200} exhibited an EMI SE value as high as 30 dB, indicating that both GP and PPy played an important role in electromagnetic shielding of the films. The principle of the films' EMI SE performance could be described as follows (Figure 8b). The electromagnetic microwave was reflected from the film surface

DOI: 10.1021/acsami.5b04462
ACS Appl. Mater. Interfaces 2015, 7, 15641−15648

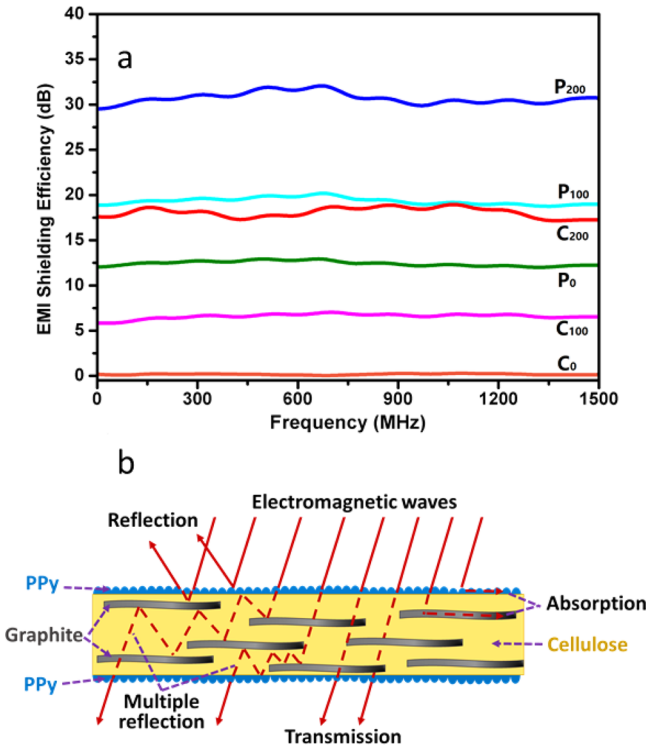

Figure 8. (a) EMI shielding effectiveness of the cellulose, cellulose/GP films before (C_0, C_{100}, C_{200}) and after (P_0, P_{100}, P_{200}) the chemical deposition of PPy, and (b) the schematic representation of shielding phenomena.

due to the impedance mismatch between PPy and air. Meanwhile, the electromagnetic energy was absorbed by the PPy and GP, resulting in the energy dissipation of electromagnetic microwave. On the other hand, the multiple internal reflection of electromagnetic radiation was occurred between the PPy coating and GP flakes because of the inhomogeneity of scattering effect within the films. Therefore, the EMI SE performance of the composite film was originated from the combination of the above three effects. As the cellulose/GP/PPy films possessed excellent thermal stability, low density, good mechanical and conductive properties, they could be considered as potential candidates for effective lightweight electromagnetic interference shielding materials in electronics, radar evasion, aerospace, and other applications.

4. CONCLUSIONS

In this study, GP powder was successfully introduced into the cellulose/PPy composite films to improve their electrical conductivity and thermal stability. The dissolution of cellulose was not influenced by the addition of GP. The XRD and FT-IR analysis confirmed the chemical structure of the composite films. The SEM and AFM images showed that the GP flakes were embedded in the cellulose matrix and the PPy nanoparticles covered the surface of the films. Although the mechanical properties of the films were decreased due to the incorporation of GP, the electoral conductivity was increased from 0.08 to 0.55 S cm^{-1}, the electromagnetic interference shielding effectiveness was improved from 12 to 30 dB, and the weight loss at 800 °C reduced from 72 to 27%. These composite films may have potential applications in electronics, radar evasion, and aerospace.

■ ASSOCIATED CONTENT

Supporting Information

Preparation process of the cellulose/GP/PPy composite films; SEM micrographs of the surface and cross-section of composite films P_0, P_{10}, P_{50}, P_{100}, and P_{200} (the part framed in P_{200} was enlarged in Figure 4a); and the excellent laundry resistance of the cellulose/GP/PPy composite film. The Supporting Information is available free of charge on the ACS Publications website at DOI: 10.1021/acsami.5b04462.

■ AUTHOR INFORMATION

Corresponding Authors

* E-mail: wangkun@bjfu.edu.cn. Phone: +86-10-62336903.
*E-mail: rcsun3@bjfu.edu.cn. Phone: +86-10-62336903.

Notes

The authors declare no competing financial interest.

■ ACKNOWLEDGMENTS

The authors are grateful for the Forestry Nonprofit Industry Research of China (201204803) and the National Science Foundation of China for the Key Projects (31430092, 31110103902).

■ REFERENCES

(1) Chiang, C.; Druy, M.; Gau, S.; Heeger, A.; Louis, E.; MacDiarmid, A. G.; Park, Y.; Shirakawa, H. Synthesis of Highly Conducting Films of Derivatives of Polyacetylene,(CH) x. *J. Am. Chem. Soc.* **1978**, *100*, 1013−1015.

(2) Balint, R.; Cassidy, N. J.; Cartmell, S. H. Conductive Polymers: Towards a Smart Biomaterial for Tissue Engineering. *Acta Biomater.* **2014**, *10*, 2341−2353.

(3) Oh, W. K.; Kwon, O. S.; Jang, J. Conducting Polymer Nanomaterials for Biomedical Applications: Cellular Interfacing and Biosensing. *Polym. Rev.* **2013**, *53*, 407−442.

(4) Tammela, P.; Olsson, H.; Strømme, M.; Nyholm, L. The Influence of Electrode and Separator Thickness on the Cell Resistance of Symmetric Cellulose-Polypyrrole-Based Electric Energy Storage Devices. *J. Power Sources* **2014**, *272*, 468−475.

(5) Shi, Y. T.; Zhan, C.; Wang, L. D.; Ma, B. B.; Gao, R.; Zhu, Y. F.; Qiu, Y. The Electrically Conductive Function of High-Molecular Weight Poly(ethylene oxide) in Polymer Gel Electrolytes Used for Dye-Sensitized Solar Cells. *Phys. Chem. Chem. Phys.* **2009**, *11*, 4230−4235.

(6) Allen, R.; Pan, L. J.; Fuller, G. G.; Bao, Z. A. Using *in-Situ* Polymerization of Conductive Polymers to Enhance the Electrical Properties of Solution-Processed Carbon Nanotube Films and Fibers. *ACS Appl. Mater. Interfaces* **2014**, *6*, 9966−9974.

(7) Dong, H.; Cao, X.; Li, C. M. Functionalized Polypyrrole Film: Synthesis, Characterization, and Potential Applications in Chemical and Biological Sensors. *ACS Appl. Mater. Interfaces* **2009**, *1*, 1599−1606.

(8) Lei, Y. H.; Sheng, N.; Hyono, A.; Ueda, M.; Ohtsuka, T. Electrochemical Synthesis of Polypyrrole Films on Copper from Phytic Solution for Corrosion Protection. *Corros. Sci.* **2013**, *76*, 302−309.

(9) Noh, K. A.; Kim, D. W.; Jin, C. S.; Shin, K. H.; Kim, J. H.; Ko, J. M. Synthesis and Pseudo-Capacitance of Chemically-Prepared Polypyrrole Powder. *J. Power Sources* **2003**, *124*, 593−595.

(10) Martel, D.; Cong, H. N.; Gautier, J. L. Induced Effect of Transparent Substrate Composition on Polypyrrole Thin Film. *J. Mater. Sci.* **2008**, *43*, 5579−5584.

(11) Nyström, G.; Mihranyan, A.; Razaq, A.; Lindström, T.; Nyholm, L.; Strømme, M. A Nanocellulose Polypyrrole Composite Based on Microfibrillated Cellulose from Wood. *J. Phys. Chem. B* **2010**, *114*, 4178−4182.

DOI: 10.1021/acsami.5b04462
ACS Appl. Mater. Interfaces 2015, 7, 15641−15648

(12) Qian, X. R.; Chen, J. H.; An, X. H. Polypyrrole-Coated Conductive Paper Prepared by Vapour-Phase Deposition Method. *Appita J.* **2010**, *63*, 102−107.
(13) Li, J.; Qian, X. R.; Chen, J. H.; Ding, C. Y.; An, X. H. Conductivity Decay of Cellulose−Polypyrrole Conductive Paper Composite Prepared by in Situ Polymerization Method. *Carbohydr. Polym.* **2010**, *82*, 504−509.
(14) Tang, L.; Han, J.; Jiang, Z.; Chen, S.; Wang, H. Flexible Conductive Polypyrrole Nanocomposite Membranes Based on Bacterial Cellulose with Amphiphobicity. *Carbohydr. Polym.* **2015**, *117*, 230−235.
(15) Liew, Soon Yee; Thielemans, Wim; Walsh, D. A. Electrochemical Capacitance of Nanocomposite Polypyrrole Cellulose Films. *J. Phys. Chem. C* **2010**, *114*, 17926−17933.
(16) Shi, Z.; Gao, H.; Feng, J.; Ding, B.; Cao, X.; Kuga, S.; Wang, Y.; Zhang, L.; Cai, J. In Situ Synthesis of Robust Conductive Cellulose/Polypyrrole Composite Aerogels and Their Potential Application in Nerve Regeneration. *Angew. Chem., Int. Ed.* **2014**, *53*, 5380−5384.
(17) Jradi, K.; Bideau, B.; Chabot, B.; Daneault, C. Characterization of Conductive Composite Films Based on TEMPO-Oxidized Cellulose Nanofibers and Polypyrrole. *J. Mater. Sci.* **2012**, *47*, 3752−3762.
(18) Takano, T.; Mikazuki, A.; Kobayashi, T. Conductive Polypyrrole Composite Films Prepared Using Wet Cast Technique with a Pyrrole-Cellulose Acetate Solution. *Polym. Eng. Sci.* **2014**, *54*, 78−84.
(19) Ge, D.; Ru, X.; Hong, S.; Jiang, S.; Tu, J.; Wang, J.; Zhang, A.; Ji, S.; Linkov, V.; Ren, B.; Shi, W. Coating Metals on Cellulose−Polypyrrole Composites: A New Route to Self-Powered Drug Delivery System. *Electrochem. Commun.* **2010**, *12*, 1367−1370.
(20) Nystrom, G.; Mihranyan, Aamir; Razaq; Lindstrom, T.; Strømme, M. A Nanocellulose Polypyrrole Composite Based on Microfibrillated Cellulose from Wood. *J. Phys. Chem. B* **2010**, *114*, 4178−4182.
(21) Wang, H.; Bian, L.; Zhou, P.; Tang, J.; Tang, W. Core−Sheath Structured Bacterial Cellulose/Polypyrrole Nanocomposites with Excellent Conductivity as Supercapacitors. *J. Mater. Chem. A* **2013**, *1*, 578−584.
(22) Olsson, H.; Berg, E. J.; Strømme, M.; Sjödin, M. Self-Discharge in Positively Charged Polypyrrole−Cellulose Composite Electrodes. *Electrochem. Commun.* **2015**, *50*, 43−46.
(23) Bober, P.; Liu, J.; Mikkonen, K. S.; Ihalainen, P.; Pesonen, M.; Plumed-Ferrer, C.; von Wright, A.; Lindfors, T.; Xu, C. L.; Latonen, R. M. Biocomposites of Nanofibrillated Cellulose, Polypyrrole, and Silver Nanoparticles with Electroconductive and Antimicrobial Properties. *Biomacromolecules* **2014**, *15*, 3655−3663.
(24) Chen, J. H.; Wang, K.; Xu, F.; Sun, R. C. Effect of Hemicellulose Removal on the Structural and Mechanical Properties of Regenerated Fibers from Bamboo. *Cellulose* **2015**, *22*, 63−72.
(25) Swatloski, R. P.; Spear, S. K.; Holbrey, J. D.; Rogers, R. D. Dissolution of Cellose with Ionic Liquids. *J. Am. Chem. Soc.* **2002**, *124*, 4974−4975.
(26) French, A. D. Idealized Powder Diffraction Patterns for Cellulose Polymorphs. *Cellulose* **2014**, *21*, 885−896.
(27) Lin, W. D.; Chang, H.-M.; Wu, R. J. Applied Novel Sensing Material Graphene/Polypyrrole for Humidity Sensor. *Sens. Actuators, B* **2013**, *181*, 326−331.
(28) Zhao, D. s.; Liu, M. s.; Ren, H. w.; Li, H.; Fu, L.; Ren, P. Dissolution of Cellulose in NaOH Based Solvents at Low Temperature. *Fibers Polym.* **2013**, *14*, 1261−1265.
(29) Yuan, L.; Yao, B.; Hu, B.; Huo, K.; Chen, W.; Zhou, J. Polypyrrole-Coated Paper for Flexible Solid-State Energy Storage. *Energy Environ. Sci.* **2013**, *6*, 470−476.
(30) Gao, W.; Alemany, L. B.; Ci, L. J.; Ajayan, P. M. New Insights into the Structure and Reduction of Graphite Oxide. *Nat. Chem.* **2009**, *1*, 403−408.
(31) Yao, L.; Lu, Y.; Wang, Y.; Hu, L. Effect of Graphene Oxide on the Solution Rheology and the Film Structure and Properties of Cellulose Carbamate. *Carbon* **2014**, *69*, 552−562.
(32) Muller, D.; Rambo, C. R.; Porto, L. M.; Schreiner, W. H.; Barra, G. M. Structure and Properties of Polypyrrole/Bacterial Cellulose Nanocomposites. *Carbohydr. Polym.* **2013**, *94*, 655−62.
(33) Hosseini, S. H.; Pairovi, A. Preparation of Conducting Fibres from Cellulose and Silk by Polypyrrole Coating. *Iran. Polym. J.* **2005**, *14*, 934−940.
(34) Varesano, A.; Tonin, C.; Ferrero, F.; Stringhetta, M. Thermal Stability and Flame Resistance of Polypyrrole-Coated PET Fibres. *J. Therm. Anal. Calorim.* **2008**, *94*, 559−565.
(35) Zhang, X.; Yan, X.; Guo, J.; Liu, Z.; Jiang, D.; He, Q.; Wei, H.; Gu, H.; Colorado, H. A.; Zhang, X.; Wei, S.; Guo, Z. Polypyrrole Doped Epoxy Resin Nanocomposites with Enhanced Mechanical Properties and Reduced Flammability. *J. Mater. Chem. C* **2015**, *3*, 162−176.
(36) Deng, F.; Min, L. J.; Luo, X. B.; Wu, S. L.; Luo, S. L. Visible-Light Photocatalytic Degradation Performances and Thermal Stability due to the Synergetic Effect of TiO_2 with Conductive Copolymers of Polyaniline and Polypyrrole. *Nanoscale* **2013**, *5*, 8703−8710.
(37) Zhao, Y.; Liu, Z.; Wang, H.; Shi, J.; Zhang, J.; Tao, Z.; Guo, Q.; Liu, L. Microstructure and Thermal/Mechanical Properties of Short Carbon Fiber-Reinforced Natural Graphite Flake Composites with Mesophase Pitch as the Binder. *Carbon* **2013**, *53*, 313−320.
(38) Cheng, W.-l.; Zhang, R.-m.; Xie, K.; Liu, N.; Wang, J. Heat Conduction Enhanced Shape-Stabilized Paraffin/HDPE Composite PCMs by Graphite Addition: Preparation and Thermal Properties. *Sol. Energy Mater. Sol. Cells* **2010**, *94*, 1636−1642.
(39) Gao, J. F.; Hu, M. J.; Dong, Y. C.; Li, R. K. Y. Graphite-Nanoplatelet-Decorated Polymer Nanofiber with Improved Thermal, Electrical, and Mechanical Properties. *ACS Appl. Mater. Interfaces* **2013**, *5*, 7758−7764.
(40) Heinze, J. r.; Frontana-Uribe, B. A.; Ludwigs, S. Electrochemistry of Conducting Polymers-Persistent Models and New Concepts. *Chem. Rev.* **2010**, *110*, 4724−4771.
(41) Efimov, O. N. Polypyrrole: A Conducting Polymer; Its Synthesis, Properties and Applications. *Russ. Chem. Rev.* **1997**, *66*, 443.
(42) Dione, G.; Dieng, M. M.; Aaron, J. J.; Cachet, H.; Cachet, C. New Composite Electrodes Made of Polypyrrole and Graphite: Construction, Optimization and Characterization. *J. Power Sources* **2007**, *170*, 441−449.
(43) Feng, X. M.; Huang, X. W.; Tan, Z.; Zhao, B.; Tan, S. T. Application Research of Polypyrrole/Graphite Composite Counter Electrode for Dye-Sensitized Solar Cells. *Acta Chim. Sin.* **2011**, *69*, 653−658.
(44) Liu, X. G.; Ou, Z. Q.; Geng, D. Y.; Han, Z.; Jiang, J. J.; Liu, W.; Zhang, Z. D. Influence of a Graphite Shell on the Thermal and Electromagnetic Characteristics of FeNi Nanoparticles. *Carbon* **2010**, *48*, 891−897.
(45) Maiti, S.; Shrivastava, N. K.; Suin, S.; Khatua, B. B. Polystyrene/MWCNT/Graphite Nanoplate Nanocomposites: Efficient Electromagnetic Interference Shielding Material through Graphite Nanoplate-MWCNT-Graphite Nanoplate Networking. *ACS Appl. Mater. Interfaces* **2013**, *11*, 4712−4724.

DOI: 10.1021/acsami.5b04462
ACS Appl. Mater. Interfaces 2015, 7, 15641−15648